U.S. DOD - Air Force Office of Scientific Research
Report Type: Final Technical Report

AFOSR Award No.: FA9550-09-1-0028
Project Period: 12/15/08 – 12/14/09

Numerical Simulation of Heliospheric Transients Approaching Geospace

Report by Dusan Odstrcil, University of Colorado, Boulder, CO

Introduction

The main aim of this one-year long project was to support graduate student's participation on the verification of numerical simulations of heliospheric transients approaching geospace. The project was supervised by Dr. Dusan Odstrcil at the University of Colorado (CU) Cooperative Institute for Environmental Sciences (CIRES) and NOAA/Space Weather Prediction Center (SWPC) at Boulder, CO. Due to late funding arrival, hiring complications emerged and Anthony Rasca, a graduate student at CU Applied Mathematics Department (and former student programmer at SWPC) was supported for shorter period than planned.

Coronal mass ejections (CMEs) have been identified as a prime causal link between solar activity and large, non-recurrent geomagnetic storms. Numerical modeling plays a critical role in clarifying the connection between solar eruptive phenomena and their impacts in the near-Earth space environment and in interplanetary space. ENLIL is the main code used for heliospheric simulations at the NSF Center for Integrated Space Weather Modeling (CISM: http://www.bu.edu/cism), at the multi-agency Community Coordinated Modeling Center (CCMC: http://ccmc.gsfc.nasa.gov), and an experimental daily-predictions tool was installed at SWPC: http://helios.swpc.noaa.gov/enlil). ENLIL was selected for transitioning to operations and thus more testing, verification, and validation is needed. This includes verification of the code initialization accuracy which plays a key role in the prediction accuracy of heliospheric transients approaching geospace.

This report presents main results achieved within the project and report by Anthony Rasca is given in Appendix. These results show significant inaccuracy in fitting the CME speeds from coronagraph observations using different techniques and were not published yet.

Numerical Modeling System

Modeling of the origin of CMEs is still in the research phases and it is not expected that real events can be routinely simulated in near future. Therefore, within our other projects, we developed a modeling system which uses the WSA coronal maps, fits coronagraph observations, specifies 3D ejecta (using the "cone" model technique), and drives the 3D numerical code ENLIL. The 3-D numerical magnetohydrodynamic code ENLIL uses the modified TVDLF (Total-Variation-Diminishing Lax-Friedrichs scheme) which has no explicit

REPORT DOCUMENTATION PAGE

Form Approved
OMB No. 0704-0188

1. AGENCY USE ONLY (*Leave Blank)*	2. REPORT DATE	3. REPORT TYPE AND DATES COVERED
		Final Report December 15, 2008 - December 14, 2009

4. TITLE AND SUBTITLE
Numerical Simulation of Heliospheric Transients Approaching Geospace

5. FUNDING NUMBERS
FA9550-09-1-0028

6. AUTHORS
Dusan Odstroil

7. PERFORMING ORGANIZATION NAME(S) AND ADDRESS(ES)
University of Colorado
CIRES
216 UCB
Boulder, Co 80309-0216

8. PERFORMING ORGANIZATION REPORT NUMBER
1540607

9. SPONSORING / MONITORING AGENCY NAME(S) AND ADDRESS(ES)
Air Force Office of Scientific Research
875 North Randolph Street
Suite 325, Room 3112
Arlington, VA 22203-1768

10. SPONSORING / MONITORING AGENCY REPORT NUMBER
FA9550-04-1-0084

11. SUPPLEMENTARY NOTES

12a. DISTRIBUTION / AVAILABILITY STATEMENT

DISTRIBUTION A: APPROVED FOR PUBLIC RELEASE

12b. DISTRIBUTION CODE

13. ABSTRACT *(Maximum 200 words)*

This one-year long project supported graduate student's participation on the verification of numerical simulations of heliospheric transients approaching geospace. Coronal mass ejections (CMEs) represent a prime causal link between solar activity and large geomagnetic storms, and numerical modeling plays a critical role in space weather research and forecasting. Numerical code ENLIL is used for heliospheric simulations at Center for Integrated Space Weather Modeling (CISM) and Community Coordinated Modeling Center (CCMC), and it was selected for transitioning to operations by NOAA Space Weather Prediction Center (SWPC). The project supported testing and verification of ENLIL in two areas. Firstly, we investigated effect of numerical resolution on interplanetary shocks. We found that while shocks are shapper and locally corrugated on very fine numerical grids, "medium" grid (radial spacing of 0.8 Rs, angular spacing of 2 deg) is sufficient for predicting arrival time of CMEs and their strength at geospace. This enables to run four simulations per day on current 32-procs systems. Finally, we investigated accuracy of the cone model fitting technique that uses coronagraph observations of CMEs and determines the location, diameter, and initial speed of ejecta launched into the heliospheric computational domain. We used multi-perspective coronagraph observations, a unique opportunity provided by NASA twin STEREO spacecraft, to verify accuracy of cone model fitting on selected CMEs. We found large differences between the initial CME speeds fitted by cone-model and stereo-model techniques but slightly smaller differences in arrival times to geospace (due to larger deceleration of faster CMEs). However, the differences between single- and multi-perspective techniques are relatively large and need to be analyzed in future.

14. SUBJECT TERMS
Space Weather
Numerical Simulations
Coronal mass ejections

15. NUMBER OF PAGES
14

16. PRICE CODE

17. SECURITY CLASSIFICATION OF REPORT	18. SECURITY CLASSIFICATION OF THIS PAGE	19. SECURITY CLASSIFICATION OF ABSTRACT	20. LIMITATION OF ABSTRACT
Unclassified	Unclassified	Unclassified	

artificial diffusion and produces second-order accuracy away from shocks and discontinuities while simultaneously providing the stability that ensures non-oscillatory solutions.

Effect of Numerical Resolution on Interplanetary Shocks

The numerical scheme must use enough grid points to ensure that properties of interplanetary shocks are not smoothed out during their propagation through huge space between the solar corona and geospace. Figure 1 shows that shocks are sharper (thinner) on finer grids but their position is basically the same. We found that “medium” numerical grid (radial spacing of 0.8 Rs (solar radius) and angular spacing of 2 deg) is sufficient for predicting arrivals of interplanetary shocks driven by CMEs and their strength at geospace. “Fine” numerical grid (0.2 Rs and 0.5 deg) provides the same predicting ability but with resolution of local shock distortions. Using “fine” grid requires huge computational resources that can be significantly reduced by using nested grids with different spacing at different regions of the computational domain; however, this approach requires more experience and time. Therefore we focused on investigation of inaccuracy in fitting the initial CME parameters from coronal observations and its effect on prediction of heliospheric disturbances.

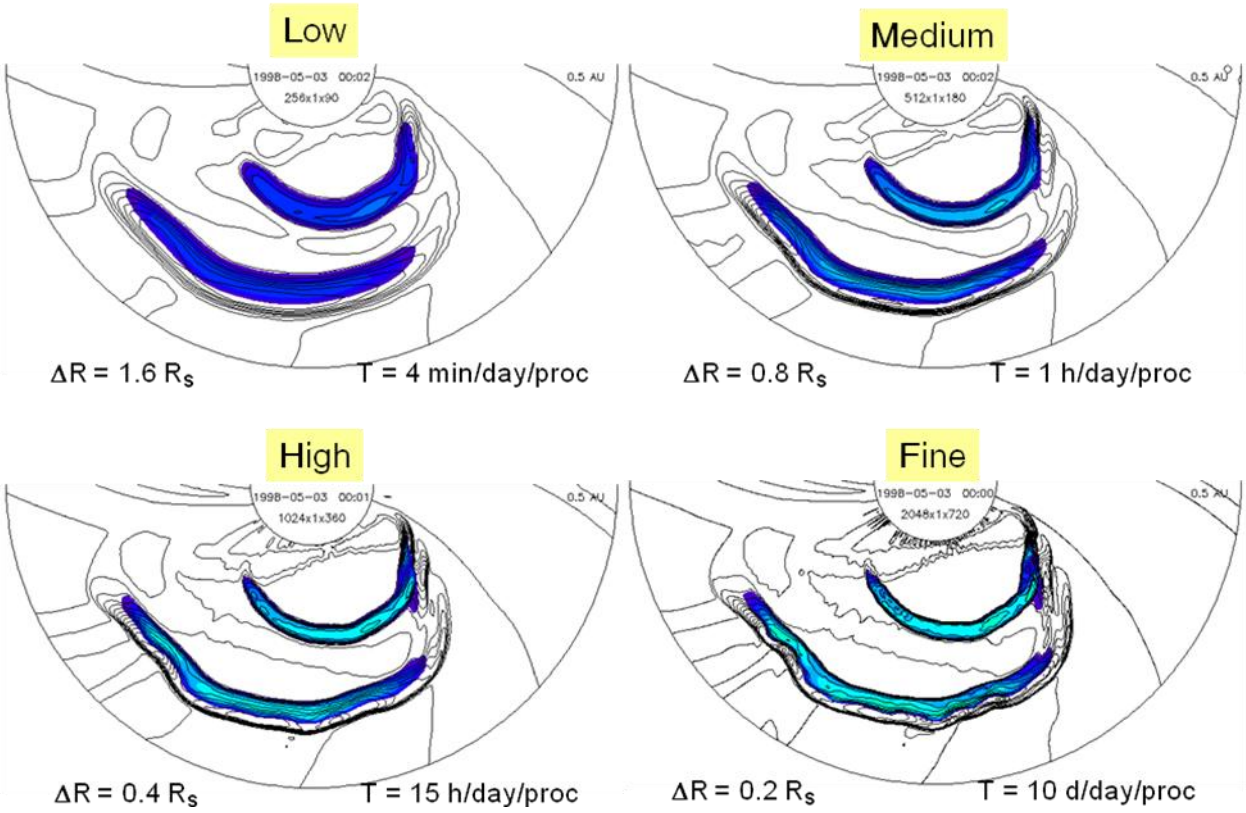

Figure 1. Two consecutive CMEs simulated by WSA+ENLIL on four progressively finer numerical grids. The normalized total (ejected material) density is shown by black contours (blue shading) on the equatorial plane. Radial grid spacing and computational resources (CPU time needed to simulate one physical day on one processor) is given at the bottom left and bottom right, respectively, on each panel.

Verification of the Cone Model Fitting Technique Accuracy

Our heliospheric space weather modeling system is based on single, near-Earth observations of CMEs that are routinely provided by NASA/ESA SOHO spacecraft. In this project, we used also multi-perspective observations of the solar corona provided by NASA STEREO spacecraft (see details in Appendix to this Report) to verify accuracy of the cone model fittings on selected CME events. The cone-model fitting enables to determine the location, speed, and angular diameter of halo CME events using single spacecraft coronagraph observations. Unless such events are very strong, their images are fuzzy which makes fitting challenging. Thus the verification and validation of the modeling system has to involve evaluation of inaccuracies in fitting procedures. Longitudinal separation of two STEREO spacecraft enabled us to use the "cone-model" and "limb-model" fitting techniques for few CME events as shown in Figure 2. We simulated propagation of interplanetary disturbances using these two sets of simulated CMEs as shown in Figures 3. We found that there are large differences in initial CME speeds (Fig. 2) and slightly smaller differences in arrival times to geospace (Fig. 2). This is caused by interaction with the background solar wind which decelerates fast CMEs and accelerates very slow CMEs. Nevertheless, these differences remain significant and inaccuracy in arrival times is up to 1-2 days. We plan to investigate ways to reduce these differences and publish the results.

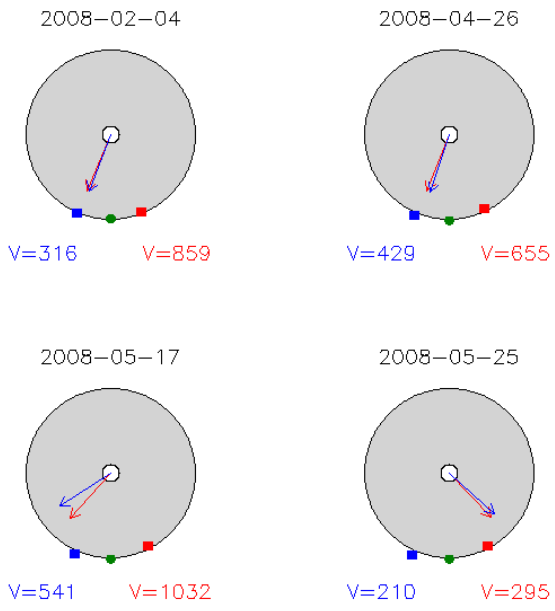

Figure 2. Overview of four CME events fitted by two different techniques using STEREO coronagraph observations. Shaded region shows the heliospheric equatorial plane with the outer boundary at 1 AU. Blue and red squares show position of STEREO spacecraft and green circle shows position of Earth. Blue and red arrows (numerical values) show the direction (initial speed) obtained by using STEREO B (blue color) and STEREO A (red color) observations.

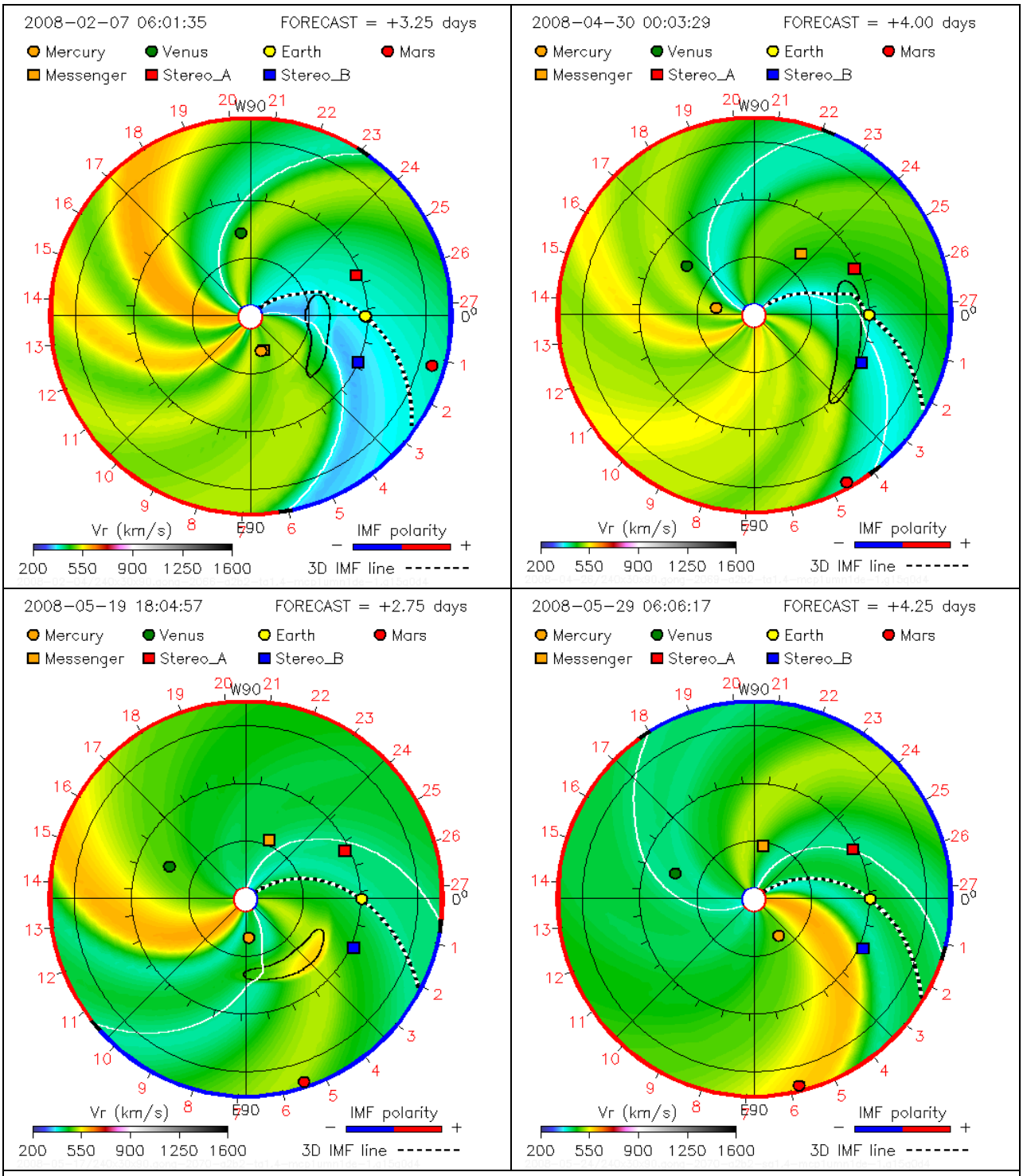

Figure 3a. Four ICME events simulated by WSA+ENLIL using the cone-model fitting technique. The radial component of the SW velocity is shown on the equatorial plane between 0.1 and 1.7 AU using the color scale given at the bottom left. The white line shows the heliospheric current sheet which represents a magnetic sector boundary with the polarity indicated by color at boundaries of the computational region; the blue is for negative (toward the Sun) and the red is for positive (away from the Sun) polarity. The black-and-white line shows the IMF line passing through Earth. Planets and spacecraft are shown by symbols as given at the top.

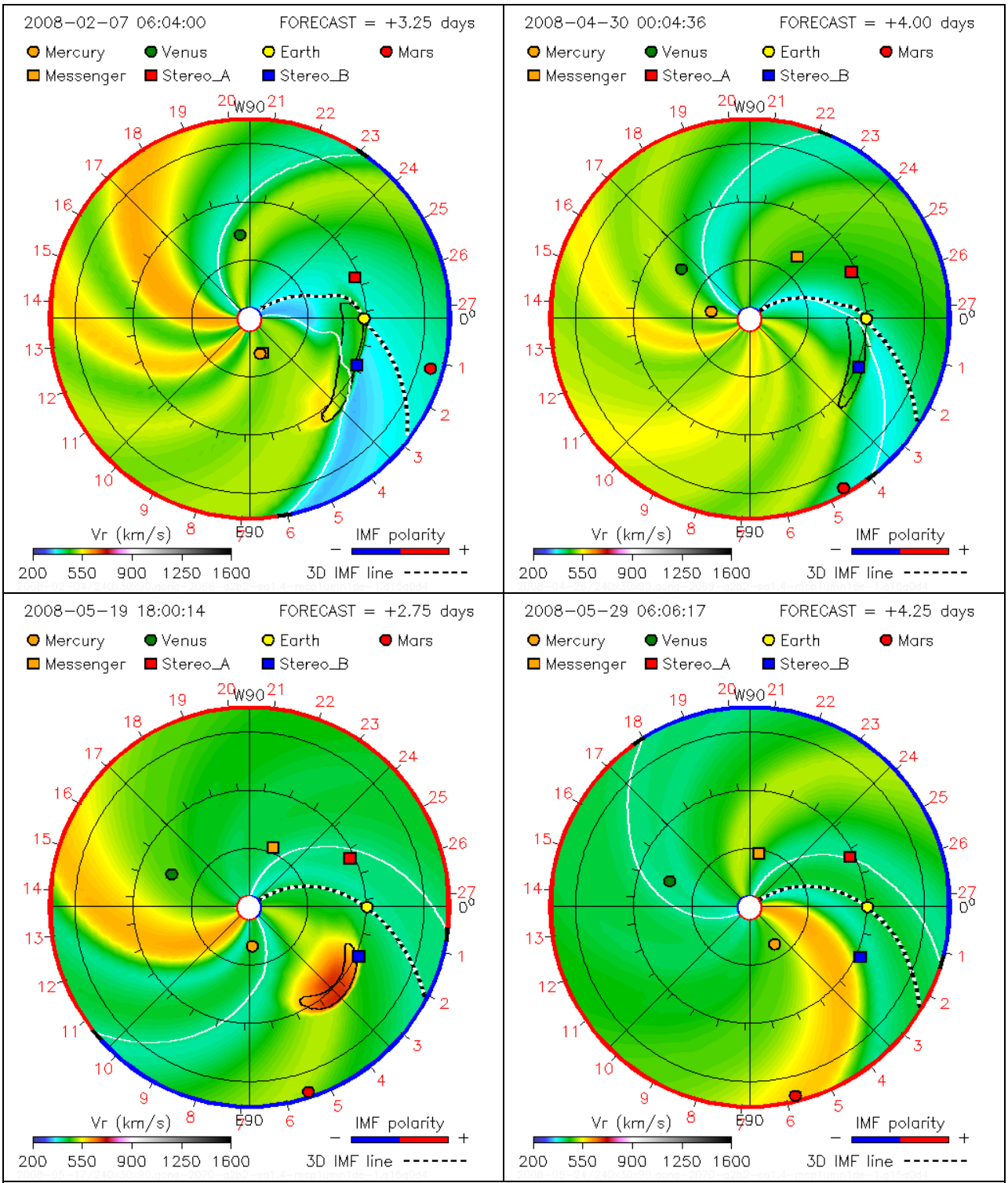

Figure 3b. Same as Fig. 3a but for numerical simulations with the initial CME parameters using the stereo-model fitting technique.

Comparing Results from Determining Halo CME Orientations using the Cone and Expansion Models

Anthony Rasca

November 30, 2009

1 Introduction

Coronal mass ejections (CMEs) pose as a major threat to artificial satellites and astronauts stationed in orbit. Though many observed CMEs tend to originate near the solar limb, their charged particles will likely never reach earth. It is the type of CME known as halo CMEs that are most capable of affecting earth. Halo CMEs appear as an expanded halo that engulfs most or all of the solar disk (Figure 1).

It is then important to determine if and when such a CME will strike the Earth's magnetosphere. Full halo CMEs are sure to affect the Earth, while CMEs with partial halos may have a small enough angular width to avoid the magnetosphere, namely an angular radius less than the difference of the CME's propagation direction and the Earth-sun line. For CMEs definitely posing as a danger, the direction of which they emanate from the solar surface will help determine the CME's radial speed which in turn helps estimate the arrival time to Earth.

This study deploys three different methods for determining the orientation of propagation for a sample of halo CMEs. The first is an iterative method that utilized two coronagraph images from different perspectives. Second, the XOL cone model, proposed by *Xie, et. al., 2006*, is used to model the expanding CME as a cone. Last, a combination of the expansion model, *Schwenn, et. al., 2005*, and simply analyzing images of the solar disk for disturbances, such as flares and prominence eruptions. Each method provides estimates on the longitude and latitude of each CME's direction of propagation relative to Earth, along with angular radius and ultimately radial speed of the leading edge.

2 Data and Methods

A sample of eight CMEs is used to test the various methods on, listed in Table 1. Our data comes primarily from the pair of STEREO satellites in orbit around the sun. The two satellites, STEREO A and STEREO B, view the sun from different angles, so we count on a CME appearing as a halo from at least one of the satellites. Table 1 notes which STEREO satellite captures the CME as a halo and which captures a near edge-on CME. The STEREO images that have halo CMEs will be used for the cone model, while the images with edge-on CMEs will be used to estimate the radial speed for the iterative and expansion models. When looking for disturbances in the solar surface, ultraviolet images of the FE XII line will be used.

2.1 Iterative Method

The iterative method compares images from the STEREO A and STEREO B satellites. Each pair of images has a CME with an identified apparent leading edge corresponding to about the same time. First a line is drawn on each image, representing the apparent angle of each leading edge (Figure 2). Another straight line corresponding to an initial guess of the longitude and latitude is then projected onto each image.

The iterative process involves carefully altering the latitude by increments of a tenth of a degree until the two lines in the image from STEREO A overlap. The longitude is then carefully adjusted until the two lines overlap in the image from STEREO B. This will more than likely result in the separation of the two lines in the STEREO A image. The process is repeated until the lines overlap in both images. The resulting longitude and latitude are then recorded as the estimated orientation of the halo CME.

With the longitude and latitude, the radial distance of the leading edge can be estimated using geometry. The same method is used after estimating the longitude and latitude from surface disturbances. For the cone model, estimating the radial distance is fortunately integrated into the actual model.

2.2 Cone Model

The cone model uses a cone to represent the propagating halo CME. The orientation, width, radial distance, and radial speed of the cone comes from fitting an ellipse to the halo CME in the satellite images. The model assumes the ellipse is a projection of the cone base. All listed cone information is then obtained using the equations from *Xie, et. al., 2004*. Even more, we also follow the XOL model, which assumes the cone axis passes through the origin. This assumption simplifies the ellipse placement process by reducing the number of ellipse parameters parameters.

2.3 Expansion Speed and Surface Disturbances

The the first of the final two methods looks at the expansion speed of halo CMEs. The expansion speed is calculated by measuring the maximum change in the halo size, perpendicular to the plane of sky velocity (Figure 3). The expansion speed is calculated between each adjacent images from both STEREO satellites. The resulting expansion speeds are then averaged. The radial speed is then estimated by multiplying the expansion speed by a factor of 0.88, as suggested by *Schwenn, et. al., 2005*. This only tells us about the radial speed and lacks any useful information on the CME's originating position.

Another way of determining the orientation of a propagating halo CME is looking at images of the solar surface. The longitude and latitude are estimated by identifying an associated solar flare, prominence eruption, or active region with a plane of sky position angle near that of the CME's leading edge. We can then take the position of the associated event on the solar disk and calculate its longitude and latitude. Also, another estimation of the radial velocity can be made with these alternative longitude and latitude values.

Images used for the associated surface event come from STEREO's EUVI 195 SECCHI camera

(Figure 4). Associated events appear bright at this wavelength. Times of the images from SECCHI depends on the time when the halo CME's shape becomes well-defined in the COR images; we looked back up to two hours before this time. Additionally, we only used images from one of the STEREO satellites. This was determined by how far from the solar limb the CME was observed propagating (position angle closer to the poles). Reasoning was that there is greater error in the position of associated event near the limb, which comes from an amplification of position uncertainty.

3 Results

Each method was attempted on each of the listed CMEs. We only say attempted because there where some CMEs where it did not appear as a halo in either STEREO image, or it may not have had an associated surface event. A general summary of results, including estimated longitude, latitude, angular radius, radial position, and radial velocity, is listed in Tables 2-9. "NA" values correspond to missing halo or associated surface event data.

We of course want estimated values for each method to be within each others' uncertainties. Agreeable results are a little hit and miss. For some halo CMEs, we can determine reasonable well which methods can be considered unreliable. For example, estimated radial velocities from the 2008-05-24 event strongly agree for the iterative (STEREO method) and associated surface event methods. Values from the other two methods are not only distant from these values, but also have very large uncertainties. In this case, we presume the cone model and expansion model are less reliable.

We now address the question, why are the cone model and expansion models useful? Well, before the STEREO satellites, we only relied on one perspective, eliminating the possibility of using the iterative method in this study. As we have seen, there are cases where there is no associated surface event, possibly implying the CME originates from the "dark" side of the sun. In these situations, cone and expansion models are must be relied on instead.

4 Conclusions

We have thus tested the iterative method, code model, associated surface event method, and expansion speed model to estimate the radial speed and orientation for a sample of halo CMEs. Not every method appears reliable; there is significant uncertainty with the cone and expansion models. However, finding associated surface events provides very accurate longitude and latitude values, which in turn gives a better radial speed estimation. Similarly, the addition of the STEREO satellites improve the quality of these estimation for a CME of any orientation.

There were of course many simplifications and assumptions made in this study. For example, we had to assume the apparent leading edge was the actual leading edge. In reality, the CME will have a more complex structure. An improvement for future studies would likely include an actual three-dimensional "light bulb" structure, similar to methods in other papers in which the parameters are modified in a similar fashion as the iterative method.

5 References

Schwenn, R., A. Dal Lago, E. Huttunen, and W. D. Gonzalez. The association of coronal mass ejections with their effects near the Earth, *Annales Geophysicae, 23, 1033-1059,2005.*

Xie, H., L Ofman, and Gareth Lawrence. Cone model for halo CMEs: Application to space weather forecasting. *J. Geophys. Res., 109, A03109, 2004.*

Improved input to the empirical coronal mass ejection (CME) driven shock arrival model from CME cone models, *J. Geophys. Res., 4, S10002, 2006.*

Table 1: Halo CMEs studied

Date	Time	Satellite[1] with halo images	Satellite[2] with edge-on images
2007-11-16	15:22:20	NA	STEREO A
	15:52:20		
2007-12-31	02:52:20	NA	STEREO A
	03:22:20		
2008-01-02	12:22:20	NA	STEREO A
	12:52:20		
2008-02-04	12:52:20	STEREO B	STEREO A
	13:22:20		
2008-04-26	17:22:20	STEREO B	STEREO A
	17:52:20		
2008-05-17	11:52:20	STEREO B	STEREO A
	12:22:20		
2008-05-24	23:52:20	STEREO A	STEREO B
	00:22:20		
2008-07-07	19:52:20	STEREO B	STEREO A
	20:22:20		

[1]images from this satellite were used with the cone model

[2]images from this satellite were used to determine radial speed with the STEREO and expansion models

Table 2: Results for 2007-11-16 event

	STEREO Model	Cone Model	Associated Surface Event	Expansion Model
Longitude	$103.3 \pm 8.3°$	NA	$113.5 \pm 3.9°$	–
Latitude	$-17.5 \pm 0.1°$	NA	$-7.7 \pm 2.7°$	–
Angular Radius	$35.5 \pm 5.5°$	NA	$33.7 \pm 4.3°$	–
R 15:22:20	11.7 ± 0.2	NA	11.6 ± 0.1	–
R 15:52:20	12.8 ± 0.2	NA	12.8 ± 0.1	–
v_r (km/s)	459.6 ± 6.6	NA	457.8 ± 3.7	325.3 ± 74.3

Table 3: Results for 2007-12-31 event

	STEREO Model	Cone Model	Associated Surface Event	Expansion Model
Longitude	$-53.0 \pm 12.7°$	NA	$-95.1 \pm 7.5°$	–
Latitude	$-9.4 \pm 2.9°$	NA	$-9.4 \pm 6.7°$	–
Angular Radius	$53.7 \pm 7.4°$	NA	$60.0 \pm 5.9°$	–
R 02:52:20	10.5 ± 0.7	NA	11.2 ± 0.7	–
R 03:22:20	13.4 ± 0.9	NA	14.2 ± 0.9	–
v_r (km/s)	1119.2 ± 72.8	NA	1192.6 ± 128.0	1071.7 ± 82.1

Table 4: Results for 2008-01-02 event

	STEREO Model	Cone Model	Associated Surface Event	Expansion Model
Longitude	$-41.1 \pm 4.7°$	NA	$-64.2 \pm 7.5°$	–
Latitude	$-9.0 \pm 2.2°$	NA	$-6.4 \pm 3.1°$	–
Angular Radius	$57.8 \pm 15.7°$	NA	$63.7 \pm 13.3°$	–
R 12:22:20	11.3 ± 0.5	NA	10.1 ± 0.1	–
R 12:52:20	13.6 ± 0.6	NA	12.1 ± 0.1	–
v_r (km/s)	885.1 ± 39.0	NA	783.0 ± 5.7	896.1 ± 277.7

Table 5: Results for 2008-02-04 event

	STEREO Model	Cone Model	Associated Surface Event	Expansion Model
Longitude	$-23.0 \pm 0.2°$	$-20.8 \pm 0.3°$	$-25.1 \pm 5.0°$	–
Latitude	$-6.9 \pm 1.2°$	$-2.7 \pm 0.3°$	$-8.5 \pm 5.5°$	–
Angular Radius	$60.5 \pm 4.3°$	$65.0 \pm 0.4°$	$61.2 \pm 4.2°$	–
R 12:52:20	16.4 ± 0.1	17.1 ± 0.1	15.9 ± 1.3	–
R 13:22:20	18.6 ± 0.1	19.4 ± 0.1	18.0 ± 1.5	–
v_r (km/s)	859.0 ± 3.0	316.1 ± 202.0	828.5 ± 2.7	556.8 ± 19.6

Table 6: Results for 2008-04-26 event

	STEREO Model	Cone Model	Associated Surface Event	Expansion Model
Longitude	$-21.4 \pm 1.1°$	$-17.8 \pm 0.5°$	$-11.1 \pm 8.1°$	–
Latitude	$14.5 \pm 0.3°$	$6.6 \pm 0.5°$	$15.6 \pm 4.4°$	–
Angular Radius	$51.7 \pm 0.7°$	$72.0 \pm 3.6°$	$46.2 \pm 0.8°$	–
R 17:22:20	16.3 ± 0.3	17.3 ± 0.2	19.8 ± 3.6	–
R 17:52:20	18.0 ± 0.3	19.1 ± 0.2	21.8 ± 4.0	–
v_r (km/s)	655.0 ± 10.9	429.2 ± 143.0	793.6 ± 19.4	566.8 ± 250.3

Table 7: Results for 2008-05-17 event

	STEREO Model	Cone Model	Associated Surface Event	Expansion Model
Longitude	$-41.9 \pm 0.7°$	$-57.0 \pm 5.4°$	$-29.4 \pm 2.6°$	–
Latitude	$-7.6 \pm 0.1°$	$-27.7 \pm 3.6°$	$-4.4 \pm 3.4°$	–
Angular Radius	$47.4 \pm 8.7°$	$84.3 \pm 2.0°$	$41.7 \pm 6.4°$	–
R 11:52:20	11.1 ± 0.1	10.4 ± 0.1	12.4 ± 0.4	–
R 12:22:20	13.8 ± 0.1	13.0 ± 0.1	15.4 ± 0.5	–
v_r (km/s)	1032.3 ± 4.7	541.0 ± 41.3	1153.3 ± 9.0	425.1 ± 121.3

Table 8: Results for 2008-05-24 event

	STEREO Model	Cone Model	Associated Surface Event	Expansion Model
Longitude	$43.6 \pm 0.4°$	$48.4 \pm 0.4°$	$43.5 \pm 3.3°$	–
Latitude	$-21.7 \pm 0.1°$	$-19.6 \pm 0.3°$	$-21.8 \pm 4.7°$	–
Angular Radius	$16.4 \pm 6.7°$	$43.6 \pm 2.8°$	$15.4 \pm 5.2°$	–
R 23:52:20	13.7 ± 0.1	13.4 ± 0.1	13.7 ± 0.3	–
R 00:22:20	14.4 ± 0.1	14.1 ± 0.1	14.4 ± 0.3	–
v_r (km/s)	294.5 ± 0.7	210.3 ± 22.3	294.6 ± 0.7	331.3 ± 148.6

Table 9: Results for 2008-07-07 event

	STEREO Model	Cone Model	Associated Surface Event	Expansion Model
Longitude	$-18.6 \pm 0.5°$	$-14.6 \pm 3.5°$	NA	–
Latitude	$-21.3 \pm 2.1°$	$-13.9 \pm 3.2°$	NA	–
Angular Radius	$26.0 \pm 0.3°$	$61.8 \pm 0.8°$	NA	–
R 19:52:20	15.3 ± 0.1	16.1 ± 0.8	NA	–
R 20:22:20	16.9 ± 0.1	17.8 ± 0.9	NA	–
v_r (km/s)	652.2 ± 4.6	233.6 ± 30.8	NA	305.3 ± 74.3

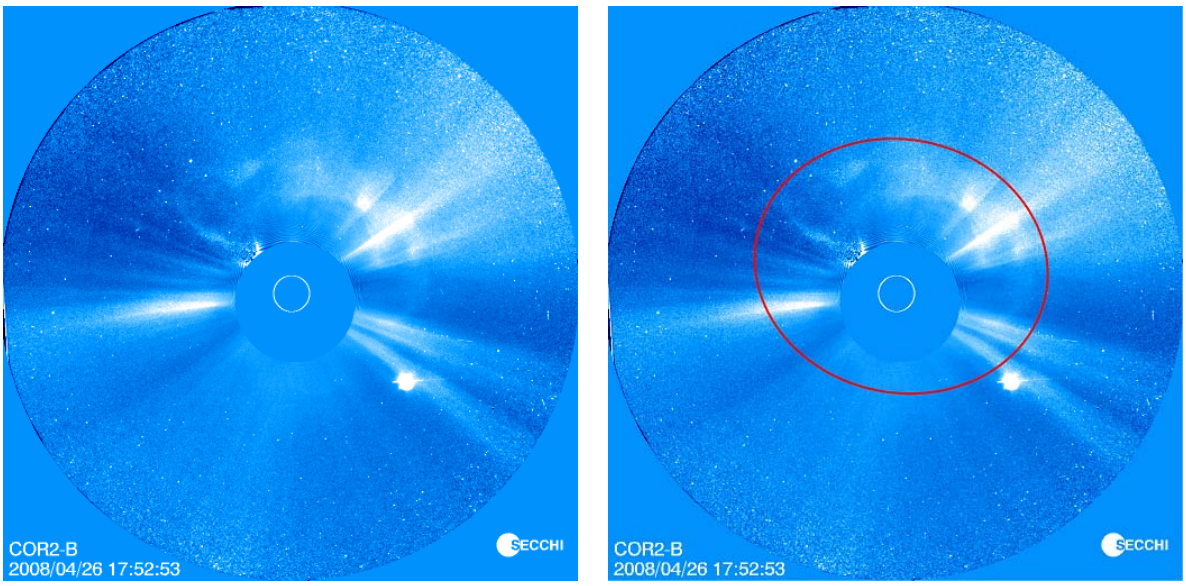

a) b)

Figure 1: a) an example of a halo CME viewed from STEREO B and b) the same image with a cone model superimposed.

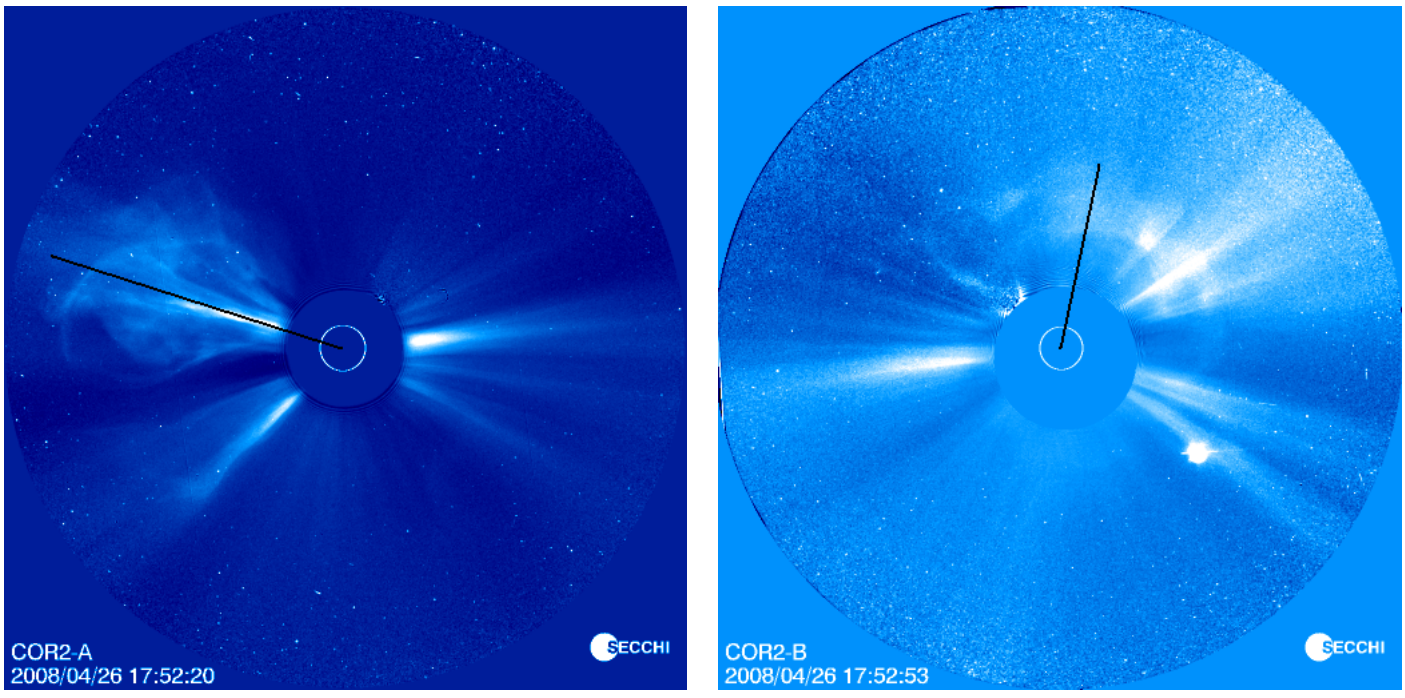

a) b)

Figure 2: modeled leading edge orientation projected onto a) the STEREO A image and b) the STEREO B image.

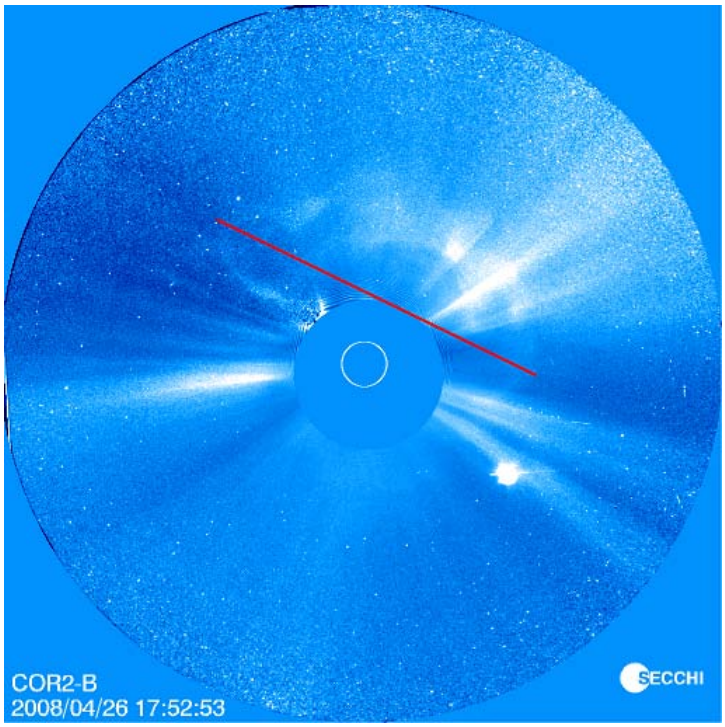

Figure 3: an example of determining the apparent expansion speed of the halo CME.

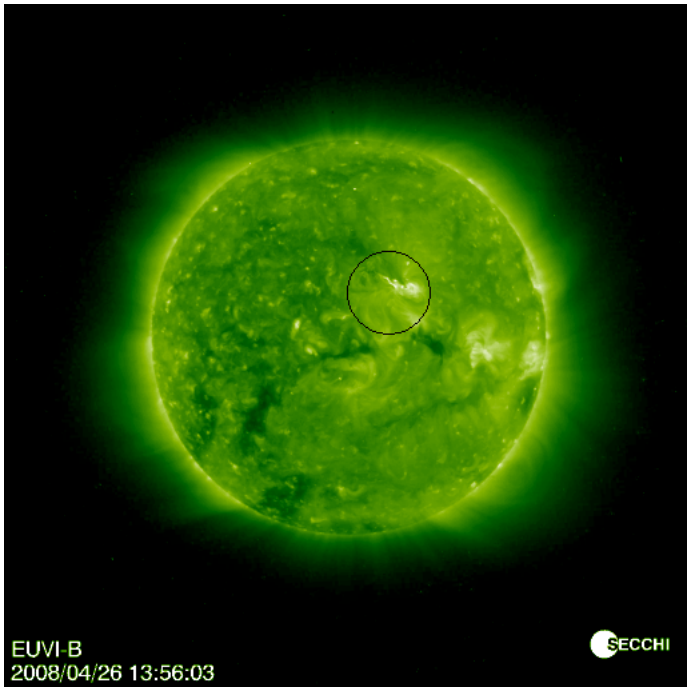

a)

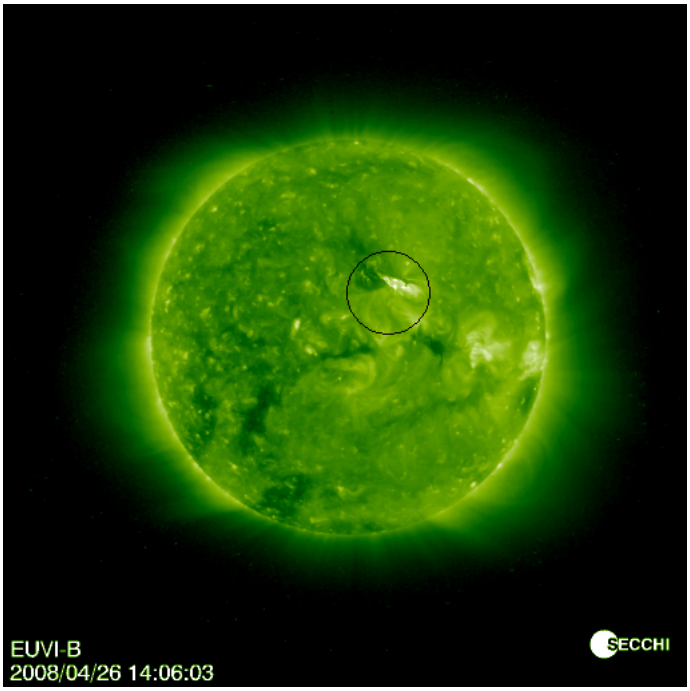

b)

Figure 4: images from the STEREO B EUVI camera representing a) before and b) after shots of an associated surface eruption.